Stress tests for a road network using fragility functions and functional capacity loss functions

Juan Carlos Lam[1,*], Bryan T. Adey[1], Magnus Heitzler[2], Jürgen Hackl[1], Pierre Gehl[3,4], Noel van Erp[5], Dina D'Ayala[3], Pieter van Gelder[5], Lorenz Hurni[2]

[1]Institute of Construction and Infrastructure Management, ETH Zurich, HIL F 27.1, Stefano-Franscini-Platz 5, 8093 Zurich, Switzerland

[2]Institute of Cartography and Geoinformation, ETH Zurich, HIL G25.1, Stefano-Franscini-Platz 5, 8093 Zurich, Switzerland

[3]Department of Civil, Environmental and Geomatic Engineering, University College London, Chadwick Building, Gower Street, London WC1E 6BT, United Kingdom

[4]Risks and Prevention Division, BRGM, 3 avenue Claude-Guillemin - BP 36009, 45060 Orléans Cedex 2, France

[5]Safety and Security Science Section, Delft University of Technology, Building 31, Jaffalaan 5, C3.310, 2628 BX Delft, The Netherlands

*Corresponding author.
E-mail addresses: lam@ibi.baug.ethz.ch (J.C. Lam), adey@ibi.baug.ethz.ch (B.T. Adey), hmagnus@ethz.ch (M. Heitzler), hackl@ibi.baug.ethz.ch (J. Hackl), p.gehl@brgm.fr (P. Gehl), h.r.n.vanerp@tudelft.nl (N. van Erp), d.dayala@ucl.ac.uk (D. D'Ayala), p.h.a.j.m.vangelder@tudelft.nl (P. van Gelder), lhurni@ethz.ch (L. Hurni)

Abstract: A quantitative approach to conduct a specific type of stress test on road networks is presented in this article. The objective is to help network managers determine whether their networks would perform adequately during and after the occurrence of hazard events. Conducting a stress test requires (i) modifying an existing risk model (i.e., a model to estimate the probable consequences of hazard events) by representing at least one uncertainty in the model with values that are considerably worse than median or mean values, and (ii) developing criteria to conclude if the network has an adequate post-hazard performance. Specifically, the stress test conducted in this work is focused on the uncertain behavior of individual objects that are part of a network when these are subjected to hazard loads. Here, the relationships between object behavior and hazard load are modeled using fragility functions and functional capacity loss functions. To illustrate the quantitative approach, a stress test is conducted for an example road network in Switzerland, which is affected by floods and rainfall-triggered mudflows. Beyond the focus of the stress test, this work highlights the importance of using a probabilistic approach when conducting stress tests for temporal and spatially distributed networks.

Keywords: stress tests; road networks; fragility functions; functional capacity loss functions; risk; post-hazard performance

This is an author generated post-print version (also known as "post-refereeing print" and "accepted manuscript") of the article:

Lam, J.C., Adey, B.T., Heitzler, M., Hackl, J., Gehl, P. , van Erp, N., D'Ayala, D., van Gelder, P., Hurni, L. (2018). Stress tests for a road network using fragility functions and functional capacity loss functions. Reliability Engineering & System Safety, 173, 78-93. 10.1016/j.ress.2018.01.015.

Note that some differences may be observed as a result of the copy-editing and typesetting process. The final manuscript is available on https://doi.org/10.1016/j.ress.2018.01.015. When citing this work, cite the final manuscript.

1. Introduction

Managers of networks (often also referred to as infrastructure; e.g., road, drinking water distribution, or power transmission) rely on a variety of methods to estimate their network-related risk (i.e., probable consequences) due to the occurrence of (natural) hazard events (e.g., floods, landslides, and earthquakes). The estimation of risk is the initial step in determining if the network would have an adequate post-hazard (physical and functional) performance—assuming that such a performance is measured in terms of risk—and if risk-reducing interventions are necessary. Examples of risk include:

- those related to physical performance such as the probable cost of restoring individual structures, which are here referred to as objects (e.g., bridges, water pipes, or transmission towers), and
- those related to functional performance such as the probable cost absorbed by society because of changes in the network's level of service, which is here referred to as network functional capacity (e.g., connectivity between two points in the network).

Quantitative risk assessment methods offer an advantage over qualitative methods: the numerical characterization of the events and their relationships needed to estimate risk, which leads to a more refined estimation. As suggested by Hackl, Heitzler [1], who built on the work of Adey, Hajdin [2], these events can be classified as source, hazard, object, network and societal events. Table 1 describes these events, and provides examples.

Event	Description	Example
Source	An event that may lead to a hazard event	• Fault rupture
Hazard	An event that may lead to an object event, and sometimes, to another (cascading) hazard event	• Strong ground-motion • Ground-motion-triggered landslides
Object	An event that represents a change in the object, which may lead to a change in network use and/or human behavior	• Bridge failure due to ground movement • Road damages due ground deformation
Network	An event that represents a change in how the network can be used, which may lead to a change in human behavior	• Loss of connectivity between two communities due to failed bridge and damaged roads
Societal	An event that represents a change in human behavior	• Restoration interventions • Re-routing of vehicles

Table 1 Classification of events and examples

Considering this classification and the use of a model to quantitatively estimate probable consequences (i.e., risk model), risk can be represented by the notation in Equation 1. This notation designates the output (Out) of the model (Mod) to be the estimated risk ($Risk$). The risk model simulates the relationships (Rel) between all the observed in the scenarios of the system state space. The system state space can be constructed/enumerated by taking the (Cartesian) product of related temporally (t) and spatially (s)

bounded source ($\overline{Scr_{t,s}}$), hazard ($\overline{Haz_{t,s}}$), object ($\overline{Obj_{t,s}}$), network ($\overline{Net_{t,s}}$) and societal ($\overline{Soc_{t,s}}$) events. Each of these—noted by an overbar—is a vector of events, or a vector of a Cartesian product of events when more than one event per category is of interest (e.g., earthquake hazard and earthquake-triggered landslide hazard). Events, and therefore scenarios, are linked to probabilities of occurrence. To accomplish this simulation, the risk model includes a number of sub-models that simulate individual events and their corresponding relationships.

$$Risk = Out\left(Mod\left(Rel\left(\overline{Scr_{t,s}} \times \overline{Haz_{t,s}} \times \overline{Obj_{t,s}} \times \overline{Net_{t,s}} \times \overline{Soc_{t,s}} \right) \right) \right) \quad 1$$

When considering a large range of possible events along with their probabilities of occurrence given a desired set of scenarios, the output risk will be a distribution—for the purpose of the following illustration, it is here assumed that a risk model can estimate a distribution like the one presented in Figure 1.

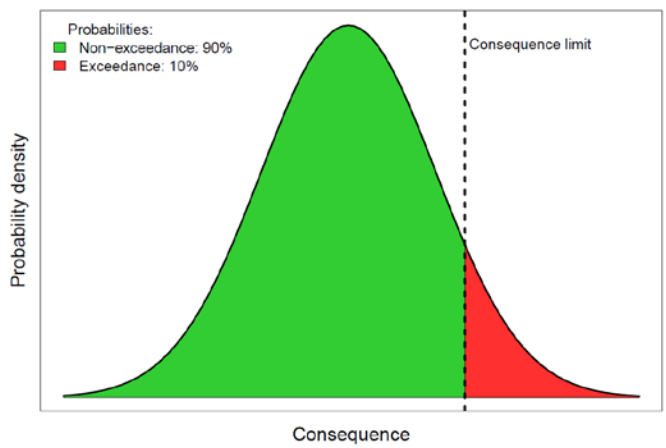

Figure 1 Illustrative risk distribution described by adequate post-hazard performance

When a network manager can describe adequate post-hazard performance for the network in terms of risk, then this information can be used to interpret the resulting risk distribution. Adequate post-hazard performance can be evaluated against:

- a consequence indicator (i.e., the type of consequence that the network manager would use to measure performance; e.g., average additional travel time per vehicle immediately after the occurrence of a hazard event, cost of repairs),
- a consequence limit [i.e., the maximum consequence that the network manager would accept to observe if a hazard event occurs; e.g., a 10% increase in the average additional travel time per vehicle within the month following the occurrence of a hazard event, cost of repairs amounting to 0.1% of the regional Gross Domestic Product (GDP)], and
- the non-exceedance probability of that consequence limit (i.e., the probability that an observed consequence resulting from a hazard event will not exceed the consequence limit; e.g., a 90% probability that at most a 10% increase in the average additional travel time per vehicle in the

month following the hazard event will be observed, a 95% probability that at most the cost of repairs will amount to 0.1% of the regional GDP).

To illustrate this, Figure 1 shows: a consequence limit (vertical dotted line) and a calculated 90% non-exceedance probability (ratio between the green area under the curve and the entire area under the curve). Given this information, network managers would need to decide whether a 90% non-exceedance probability means that risk-reducing interventions should be executed, or not.

When the composition of the risk model changes, then the network manager can expect to obtain a different risk distribution, and therefore, observe a different consequence limit non-exceedance probability. Changes can occur when network managers are seeking to:

- reduce the uncertainty of the results due to improved knowledge, for example:
    - the execution of a traffic load analysis to determine the load carrying capacity of a bridge in the network after a simulated earthquake event rather than the use of a capacity heuristically approximated by experienced bridge engineers when computer support increases, or
    - the replacement of a macro traffic sub-model for a micro traffic sub-model when the resolution of the analysis is part of a city and more data are available, or
- better quantify the uncertainty, for example:
    - the consideration of a larger number of possible hazard events by extending the maximum considered return period,
    - the random application of interchangeable ground motion prediction equations (GMPEs) during the modeling of the earthquake event, or
    - the characterization of the number of available crews for post-hazard restoration interventions by a probability distribution instead of using an expected quantity.

In these cases, which this work refers to as model updating, the consequence limit should remain the same despite changes in the estimated risk. Figure 2 shows the illustrative distribution with reduced uncertainty as well as the reevaluation of risk based on the same consequence limit. It is here observed that the new consequence limit non-exceedance probability is 97%. This means that network managers may be now more inclined to not execute interventions to reduce risk.

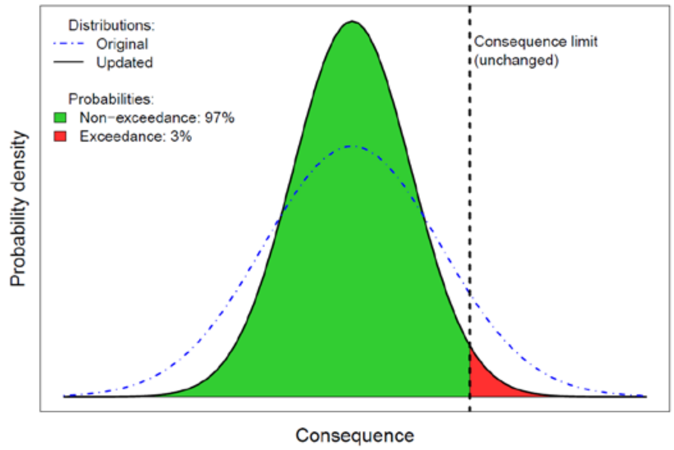

Figure 2 Illustrative updated risk distribution

A network manager can also change a risk model by representing at least one uncertainty (i.e., an uncertain element of the risk model; i.e., events, relationships, parameters) with a subset of probable values (i.e., a probable realization of the uncertain element). This work refers to this process as model conditioning. Clear examples include, but are not limited to the following (note the parallel between these examples and those cited previously when referring to improving the quantification of uncertainty):

- the selection of specific events resulting in changes to the scenario space (e.g., including only low-probability, high-consequence hazard events),
- the integration of a sub-model that gives more conservative or less conservative relationships (e.g., using a GMPE that generally provides the most conservative results for short distances when the area of concerned is near the modeled seismogenic source), and
- the use of upper or lower bound uncertain parameters, or parameters from a distribution that match a specific percentile (e.g., using the minimum number of crews thought to be available for post-hazard restoration interventions).

When conditioning a model, a network manager should expect to obtain a different risk distribution, and therefore, determine the new consequence limit and non-exceedance probability of that consequence limit based on the conditions applied to the model. For example, generally, the consequence limit for a hazard event with a 50-year return period should not be the same as the consequence limit corresponding to a hazard event with a 500-year return period. This is illustrated in Figure 3. It is observed that when conditioned, the risk model, along with the changed consequence limit, leads to a consequence limit non-exceedance probability of 85%. This means that network managers may be now more inclined to actually execute an intervention to reduce risk. Possible new consequence limits will depend on the infrastructure sector and the priorities and contexts of the network managers in addition to the conditions applied to the risk model.

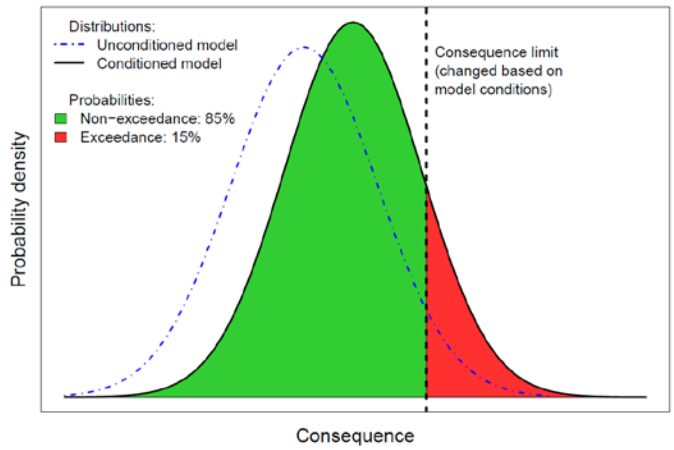

Figure 3 Illustrative conditioned risk distribution

The next section presents an approach for conducting a special type of assessment that uses conditioned risk models. These assessments are referred to as stress tests. The general approach is consistent with the work of van Erp, Linger [3] and van Erp, Linger [4], who, from a probability theoretical point of view, stated that stress tests involve the construction of conditional consequence probability distributions. Considering that networks are temporal and spatially distributed, a probabilistic approach helps to account for the possible ways events can occur over time and space (e.g., a hazard event of a given return period can manifest in various ways over a geographic area). A deterministic approach (here defined as an approach that aims at evaluating the adequacy of the post-hazard performance of a network based on a specific scenario; i.e., one combination of events) presents limitations on this regard and the decision on whether to intervene or not depends heavily on the selection of the scenario.

The next section moves from a general approach to conducting stress tests to a more specific one that focuses on using risk models, whose conditions are related to the uncertain behavior of individual objects that are part of a network when subjected to hazard loads. An example is then presented to demonstrate the application of the specific stress test approach. The example includes:

- a short introduction to the problem statement,
- an overview of the risk model,
- the definition of the stress test conducted,
- descriptions of the functions used to relate object behavior and hazard load,
- an overview of the additional key data needed to understand the outputs of the risk model,
- the estimated risk of the stress test conducted, and
- an evaluation to determine the need to execute risk-reducing interventions.

This work closes with a discussion on the application of the approach and a summary of the work and an outline of future research steps.

This is an author generated post-print version (also known as "post-refereeing print" and "accepted manuscript") of the article:

Lam, J.C., Adey, B.T., Heitzler, M., Hackl, J., Gehl, P. , van Erp, N., D'Ayala, D., van Gelder, P., Hurni, L. (2018). Stress tests for a road network using fragility functions and functional capacity loss functions. Reliability Engineering & System Safety, 173, 78-93. 10.1016/j.ress.2018.01.015.

Note that some differences may be observed as a result of the copy-editing and typesetting process. The final manuscript is available on https://doi.org/10.1016/j.ress.2018.01.015. When citing this work, cite the final manuscript.

It is worth noting that stress tests have been commonly used in non-infrastructure sectors (e.g., financial and healthcare) and sometimes used in infrastructure sectors (e.g., nuclear and transport) to model and evaluate adverse outcomes, not necessarily risk due to hazard events. For example, Li, Yu [5] and Mercier, Crozet [6] applied stress tests to estimate the sufficiency of network flow capacities and changes in mobility behavior. Furthermore, Lambert, Tsang [7], You, Connelly [8], Hamilton, Lambert [9] and Thorisson, Lambert [10] applied various types of stress tests to:

- estimate the performance of portfolios of highway equipment, highway, coastal flood risk and storm damage reduction, and electric power projects, respectively,
- determine the implied changes in the prioritization of these projects, and
- identify the critical stress tests based on their assessed impacts.

Avdeeva and van Gelder [11] compiled a list of stress tests conducted in various sectors. Only one set of examples found in the literature review relates to the work presented here because of its focus on hazards: the post-Fukushima stress tests conducted at individual European Union nuclear power plants [12]. The European Nuclear Safety Regulators Group [13] described the specifications of the deterministic stress tests conducted for European Union nuclear power plants.

2. Stress tests

2.1. General approach

A stress test is a quantitative assessment designed to evaluate the ability of a network to perform adequately during and after the occurrence of hazard events, where the assessment is conducted using a risk model that is conditioned on representing at least one uncertainty in the model with values that are considerably worse than the corresponding median or mean values. The characteristic "considerably worse" implies that the selected values would lead to a significantly larger risk estimation. On purpose, this characteristic is not further qualified here to acknowledge that the task of selecting the values to use in a stress test belongs to the network manager.

The conditions imposed on the risk model demand an understanding of the physical system being analyzed to determine the continued adequacy of the remaining elements of the model (e.g., when conditioning the risk model to estimate the risk due to high-consequence, low-probability hazard events, it is necessary to evaluate whether the hazard model used in the original model is still a suitable model to simulate such hazard events). Moreover, in establishing the conditions to the risk model, it should be kept in mind that an increasing number of conditions, in general, decreases the ability of the network manager to consider uncertainties, and therefore, increases the difficulty to determine suitable post-hazard performance evaluation criteria.

Post-hazard performance is still evaluated against a consequence indicator, a consequence limit, and the non-exceedance probability of that consequence limit. As in the case of model conditions, this work

This is an author generated post-print version (also known as “post-refereeing print” and “accepted manuscript”) of the article:

Lam, J.C., Adey, B.T., Heitzler, M., Hackl, J., Gehl, P. , van Erp, N., D'Ayala, D., van Gelder, P., Hurni, L. (2018). Stress tests for a road network using fragility functions and functional capacity loss functions. Reliability Engineering & System Safety, 173, 78-93. 10.1016/j.ress.2018.01.015.

Note that some differences may be observed as a result of the copy-editing and typesetting process. The final manuscript is available on https://doi.org/10.1016/j.ress.2018.01.015. When citing this work, cite the final manuscript.

provides no prescribed guidance on the selection of appropriate evaluation criteria as this activity also belongs to the network manager. It is plausible to imagine, however, that network managers will select:

- consequence indicators and consequence limits that are aligned with strategic goals, contractual agreements, and policies and regulations, among others, and
- a large non-exceedance probability of the consequence limit (e.g., two-standard deviations) to reflect a level of certainty conducive to firm decisions on whether or not to plan and execute risk-reducing interventions.

Finally, in cases where there is a need to consider more than one consequence indicator, these need to be explicitly explained. This may occur when needing to (i) evaluate multiple performance measures, (ii) disaggregate the results of a given performance measure (e.g., for each cascading hazard, for each part of network, for each network category), or (iii) evaluate multiple non-cascading hazard events. The following is an example. Two consequence indicators are of interest: (i) the average additional travel time per vehicle in the month following the occurrence of a hazard event on high-speed roads, and (ii) the average additional travel time per vehicle in the month following the occurrence of a hazard event on local roads. The consequence limit is set to be 10% for additional travel time on high-speed roads, or 20% for additional travel time on local roads. The non-exceedance probability is 90% for both cases. The network manager also has the following additional combined post-hazard performance evaluation criteria: a 90% probability that at most a 5% for additional travel time on high-speed roads and a 15% for additional travel time on local roads are observed at the same time.

2.2. Stress tests using fragility functions and functional capacity loss functions

The specific type of stress tests presented in this work is focused on the uncertain behavior of individual objects that are part of a network when these are subjected to hazard loads. One of the conditions imposed on the risk model is to represent in a quantitative manner this uncertain hazard-object relationship using upper-percentile fragility functions and functional capacity loss functions rather than the respective median functions, which is a common practice in risk assessments. The usefulness of conditioning a risk model in this manner is that, once the stress test is passed, the network manager has an increased confidence that actual consequences will likely not exceed the accepted limit. In other words, conditioning helps to take into consideration potential deviations in the modeling of network performance, serving a similar purpose to that of safety factors in structural engineering.

Fragility functions relate hazard intensity measures to the probabilities of meeting or exceeding a specific object damage state. These functions are widely used in risk assessments, including those concerning road networks (e.g., Clarke, Lam [14]). A set of functions is illustrated in Figure 4, where three damage states are defined. Fragility functions have been extensively researched by several authors, including D’Ayala, Gehl [15], Porter [16] and Rossetto, Ioannou [17].

This is an author generated post-print version (also known as "post-refereeing print" and "accepted manuscript") of the article:

Lam, J.C., Adey, B.T., Heitzler, M., Hackl, J., Gehl, P. , van Erp, N., D'Ayala, D., van Gelder, P., Hurni, L. (2018). Stress tests for a road network using fragility functions and functional capacity loss functions. Reliability Engineering & System Safety, 173, 78-93. 10.1016/j.ress.2018.01.015.

Note that some differences may be observed as a result of the copy-editing and typesetting process. The final manuscript is available on https://doi.org/10.1016/j.ress.2018.01.015. When citing this work, cite the final manuscript.

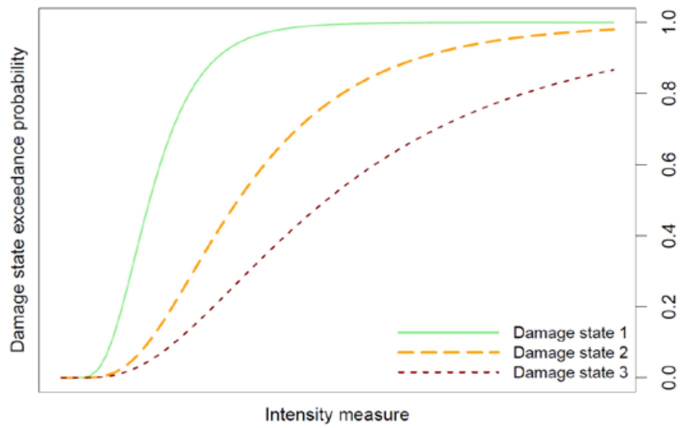

Figure 4 Illustrative fragility functions

Functional capacity loss functions relate hazard intensity measures to various losses in levels of service provided by objects. An illustrative functional form is presented in Figure 5, and specific examples can be found in Lam and Adey [18]. In that work, a distinction is made between (i) initial functional capacity loss, which represents the loss during the hazard event period and the initial part of the restoration period until a restoration intervention is executed, and (ii) functional capacity loss during restoration, which represents the loss during the execution of the restoration intervention (e.g., closure of a bridge for repairs). This family of functions is less common than fragility functions. Most works that have sought to establish a direct relationship between loss of level of service and hazard intensity measures have limited this relationship to be represented by binary or step functions (e.g. Kermanshah, Karduni [19]).

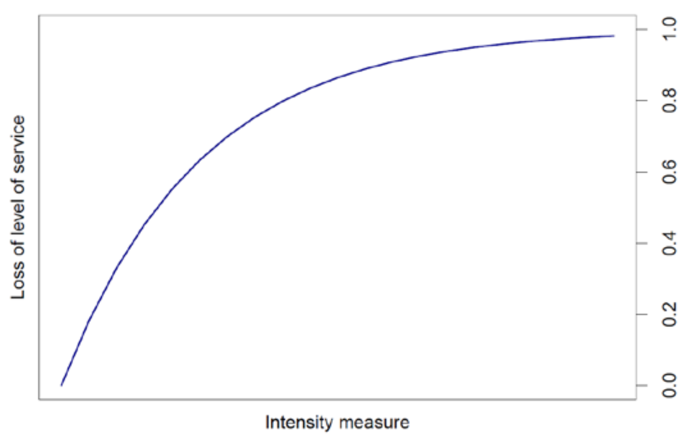

Figure 5 Illustrative functional capacity loss function

Fragility functions and functional capacity loss functions as those presented in Figure 4 and Figure 5 are the median representations of an uncertain relationship between hazard events and object events. Figure

6 displays illustrative bounds for unspecified upper and lower-percentiles. Sources of uncertainty include, but are not limited to:

- estimating the behavior of the object when subjected to a hazard load (e.g., the type of seismic analysis for a network bridge),
- modeling the uncertain parameters required to simulate the response of the object (e.g., the probability distribution thought to describe the value of a parameter),
- defining the damage states in the case of fragility functions [e.g., (i) damage states based on determined functional capacity losses, (ii) object element and/or damage measure that help(s) describe the damage states, and (iii) damage state thresholds for the chosen damage measure], and
- fitting the resulting damage state exceedance probabilities and loss of level of service (e.g., the probability distribution thought to describe the form of the function).

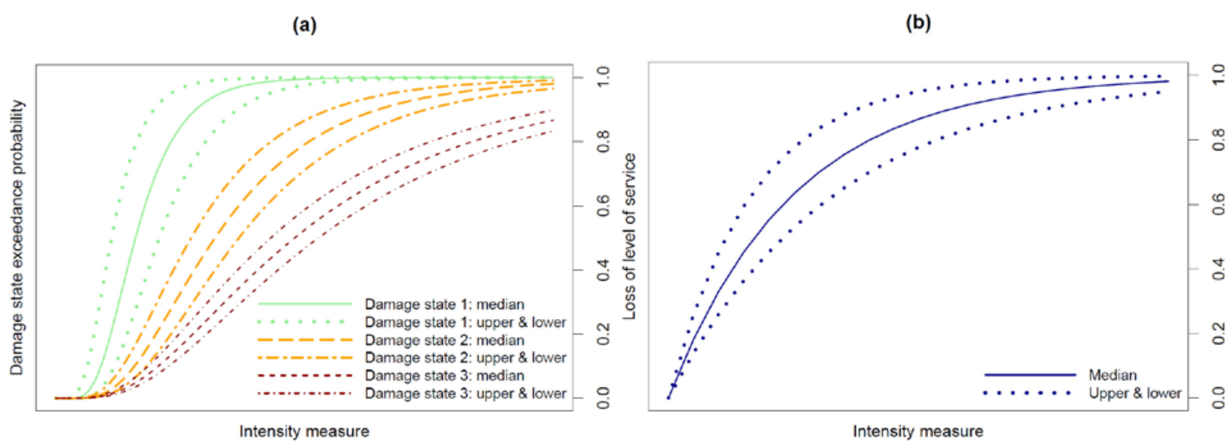

Figure 6 Illustrative (a) fragility functions and (b) functional capacity loss function with uncertainty bounds

The use of upper-percentile functions in stress tests leads to an increase in damage state exceedance probabilities and in loss of service, which at the same time lead to an increased risk estimation. As described here, fragility functions and functional capacity loss functions have not been used previously in stress tests for road networks.

An example upper percentile is 95. This is the percentile used in the estimation of the high-confidence low-probability failure (HCLPF) capacity of selected nuclear power plant elements as part of a plant seismic margin assessment. HCLPF capacity is an indicator of the level of seismic safety of an element and is equivalent to the seismic intensity measure that corresponds to a 5% exceedance probability of plant failure (damage state) when using the 95-percentile fragility function that describes the probability of plant failure [20]. While the consequences of road network failure are not considered larger than those of nuclear power plants, using 95-percentile fragility functions and functional capacity loss functions could be justified for road networks knowing the critical services that these networks provide during and after a hazard event. These services include mobilizing human and physical resources to respond to failures in interdependent sectors (e.g., nuclear, industrial) that can lead to even larger consequences, not mentioning the importance of an operational road network to transport population in need of medical attention and recover economic losses.

3. Example definition

3.1. Introduction

The example demonstrates how a road network manager can first develop a risk model for a road network with a probability of being affected by floods and rainfall-triggered mudflows using the risk model of Hackl, Heitzler [1]. Then, the example shows how the network manager can define and implement a stress test by choosing to model hazard events of a specific return period and using 95-percentile fragility functions and functional capacity loss functions.

3.2. Problem statement

The Rhine Valley area around Chur, Switzerland in the Canton of Grisons was suspected to have a road network with inadequate performance when subjected to floods and rainfall-triggered mudflows. Historical records and previous studies suggest that these hazards are of high concern. The road network in the area of study, which plays an important role in the economy of the eastern part of Switzerland, consists of 32 km of high-speed roads, 559 km of local roads (primary roads and roads of lower category), and 92 bridges, with many of these objects exposed to the hazards of interest.

Loads related to flooding may be categorized as hydrostatic, hydrodynamic and impact [21]. These loads can be similarly associated with specific object events: inundation, bearing capacity degradation (hydrostatic), scour, erosion and hydraulic loading (hydrodynamic) and debris impact (impact) [22]. Loads generated by landslides depend on the type of landslide (e.g., falls, topples, flows, spreads) and material (e.g., rocks, soil, mud). Resulting object events range from obstruction to destruction, with potential damages to various non-structural and structural elements. The types of object events in this example are: (i) bridge local scour (at piers only), (ii) road section mudflow-blocking (i.e., blockage of a road section due to mudflow deposits), and (iii) road section inundation, all of which had been observed in the area of study.

3.3. Risk model

The detailed quantitative and computer-supported model used to estimate the road network-related risk is described in Hackl, Heitzler [1]. Here, only a summary of the risk model (with an improved workflow) is introduced.

This is an author generated post-print version (also known as "post-refereeing print" and "accepted manuscript") of the article:

Lam, J.C., Adey, B.T., Heitzler, M., Hackl, J., Gehl, P. , van Erp, N., D'Ayala, D., van Gelder, P., Hurni, L. (2018). Stress tests for a road network using fragility functions and functional capacity loss functions. Reliability Engineering & System Safety, 173, 78-93. 10.1016/j.ress.2018.01.015.

Note that some differences may be observed as a result of the copy-editing and typesetting process. The final manuscript is available on https://doi.org/10.1016/j.ress.2018.01.015. When citing this work, cite the final manuscript.

3.3.1. Events and spatial and temporal boundaries

The events included in the risk model along with their temporal boundaries are presented in Table 2. In the model, there were two distinctive time periods: (i) during hazard events, and (ii) during restoration. The length of the former period was determined by the modeling of the source and hazard events (in hourly time units). Object events, network events and societal events were also modeled during the hazard events period to evaluate the performance of the road network. The restoration period occurred once the hazard event period ended, and continued until all objects in need of a restoration intervention were restored to their original condition (in daily time units). During the restoration period, network and societal events were modeled. The period of analysis was assumed to last one full year, and within this period, a maximum of one scenario was considered to occur.

Event category	**Types of events**	**Temporal boundary**
Source ($\overline{Scr_{t,s}}$)	• Rainfall events of return periods ranging from 1 to 10,000 years	• Rainfall events were considered to fall within the period of analysis of one year. These events were assumed to last no more than three days.
Hazard ($\overline{Haz_{t,s}}$)	• Floods • Mudflows	• The duration of the floods was determined by the rainfall-runoff-flood sub-model, with the flood being attributed to the Rhine and the Hinterrhein only. • Mudflows were only triggered during the rainfall event (i.e., within the maximum three day period).
Object ($\overline{Obj_{t,s}}$)	• Bridge local scour • Mudflow-blocked road section • Inundated road section	• These events were triggered during the hazard events. • Road sections were no longer inundated immediately after a flood event (i.e., flood water dissipated), but some were marked as needing restoration depending on the inundation level experienced during the hazard events period.
Network ($\overline{Net_{t,s}}$)	• Time-varying network functional capacity	• Network events such as reduced road network capacity and speed as well as loss of connectivity occurred during the hazard events period, and were later updated during the restoration period.
Societal ($\overline{Soc_{t,s}}$)	• Restoration of objects • Traffic changes	• Restoration period began after the occurrence of hazard events, and ended when all objects in need of restoration were restored. • Vehicle travel/missed trips occurred during the hazard events and restoration period.

Table 2 Events

The spatial boundaries of the selected events are shown in Figure 7.

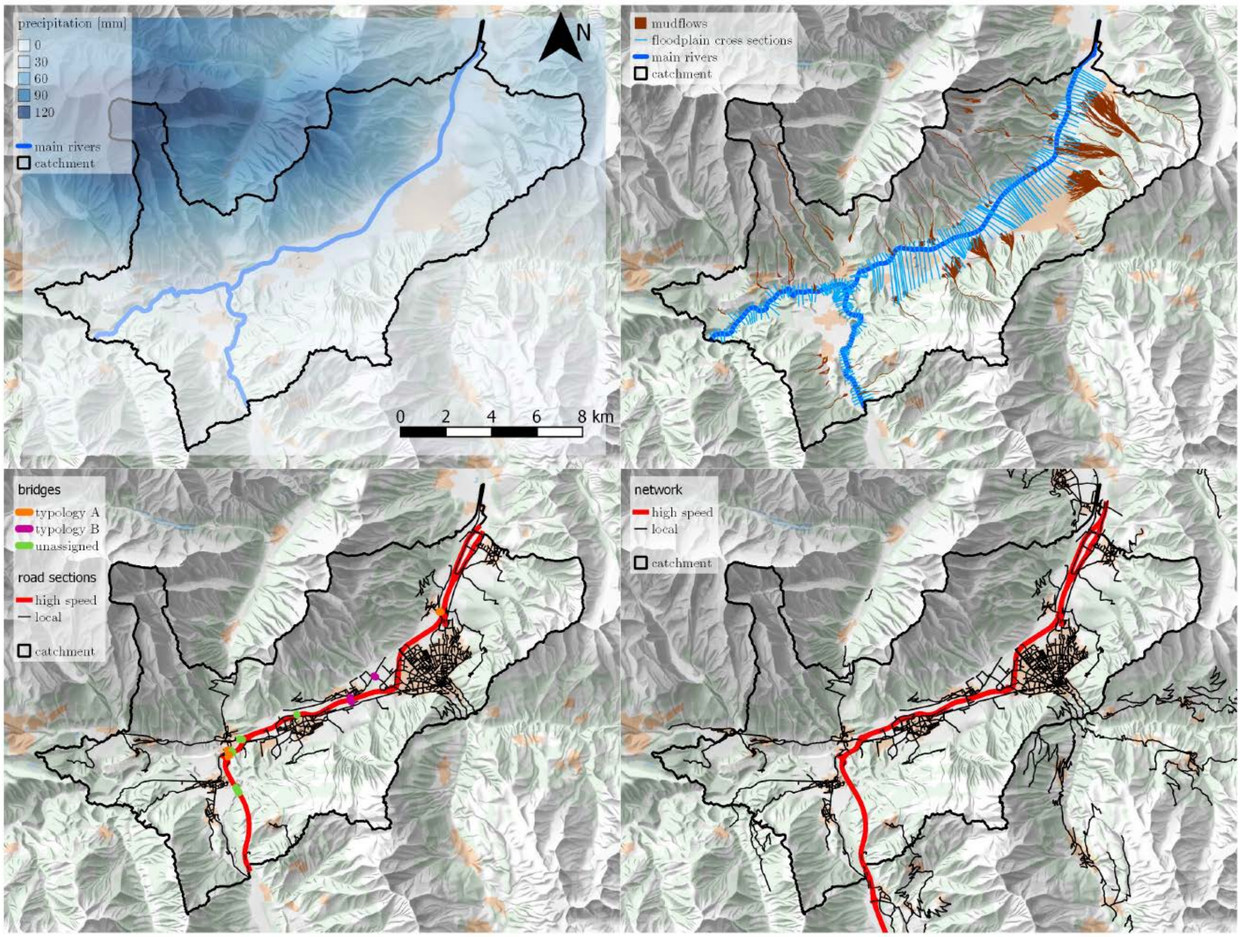

Figure 7 Spatial boundaries of events: source (top left), hazard (top right), object (bottom left), network and societal (bottom right)

3.3.2. Relationships and scenarios

The relationships linking the selected events into scenarios are described in Table 3. Scenarios, as defined earlier, were built based on the combination of the events listed in Table 2. A given rainfall event resulted in floods as well as cascading mudflows given the estimations of a runoff sub-model and the application of a rainfall intensity-duration function, respectively. The hazard events, which were represented by spatio-temporally-distributed intensity measures, resulted in a series of levels of bridge local scour, mudflow-blocked road sections and inundated road sections, which were estimated through the application of fragility functions and functional capacity loss functions. The network functional capacity at various time steps was determined based on the estimated conditions of individual objects and the network topology, which helped spatially connect these objects. At the end of the hazard events period, restoration interventions were simulated to be executed. The order of execution was determined based on least expected restoration time (i.e., the intervention that was the fastest to complete was executed first). This criterion was used as a proxy for improvement in network functional capacity. It was assumed that multiple interventions could be executed at the same time, depending on the number of work crews. Throughout the hazard event period and restoration period, and therefore, at various network functional capacity states, traffic changes—measured in terms of additional travel time and missed trips—were modeled with the aid of an Origin-Destination matrix that related vehicle flow to the changing road network. A total of 1,180 scenarios were modeled as part of the original risk assessment.

Relationship category	**Types of relationships**
Source-Hazard	• Runoff for floods to estimate how much rainfall could not be absorbed by the environment, affecting river discharge • Intensity-duration function for the cascading mudflows to determine the combination of rainfall intensity and duration needed to trigger mudflows
Hazard-Object	• Fragility functions for bridge local scour that related river discharge with the probability of reaching or exceeding a given damage state • Fragility functions for mudflow-blocked road sections that related mudflow volume with the probability of reaching or exceeding a given damage state • Functional capacity loss functions for inundated road sections that related inundation depth with a feasible speed
Object-Network	• Network topology to understand how objects were spatially connected and how functional capacity losses were to be aggregated from the object level to the network level
Object-Societal	• Restoration prioritization based on the condition of individual objects to schedule the needed restoration interventions
Network-Societal	• Origin-Destination matrix to understand which vehicles were moving, and where these were starting their trips and where these were traveling to

Table 3 Relationships

3.3.3. Sub-models

Figure 8 and Figure 9 illustrate the workflow of the risk model using Business Process Model and Notation. The hazard sub-models (Figure 8) included three different sets of activities. The first set (highlighted in dark green) consisted of initially modeling a series of rainfall events using pre-determined spatio-temporal precipitation fields from Wüest, Frei [23], as well as the resulting runoff and discharge scenarios using the ModClark model [24]. The second set of activities (highlighted in dark blue) determined whether the resulting discharge scenario corresponded to the discharge value of a desired return period, which was estimated based on available gauge data. Calibration of the rainfall event (i.e., upscale, downscale of pre-determined spatio-temporal precipitation fields) was executed if the desired return period was not achieved. The third set of activities (highlighted in dark red) completed the modeling of the hazard by simulating the flood event using a 1D steady and gradually-varied flow model, as well as the cascading mudflow events using geometries from Losey and Wehrli [25] and an intensity-duration function from Zimmermann, Mani [26]. More details on the sub-models can be found in Hackl, Heitzler [27].

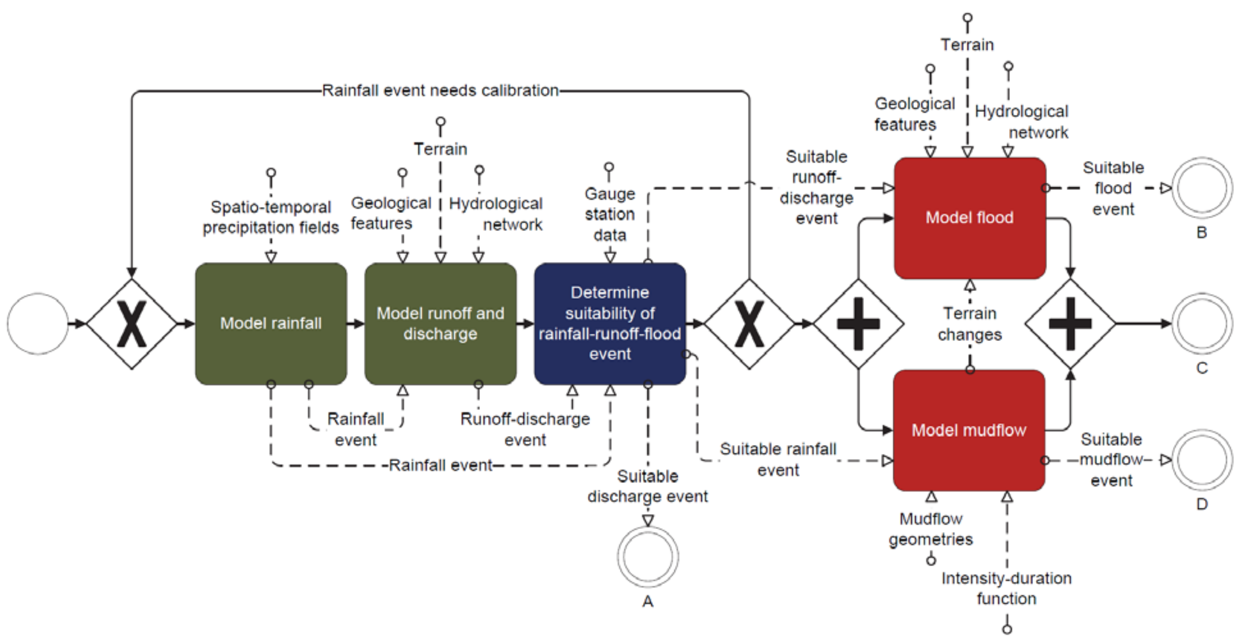

Figure 8 Hazard sub-models

The damage and consequence sub-models (Figure 9) included four distinctive groups of activities. The first group (highlighted in light gold) obtained the output intensities of the hazard events to estimate (i) the probabilities of objects being in different damage states using fragility functions, and (ii) the reduction of speed for inundated roads using functional capacity loss functions. For bridge local scour and road section mudflow-blocking, the probabilities of damage states along with estimations of corresponding functional capacity losses, restoration times and costs (i.e., referred to as consequence parameters in Figure 9) were used as indicated by Lam and Adey [18] to determine expected restoration cost, restoration time and functional capacity loss estimates at the object level. For road section inundation, reduction of speed along with estimated restoration times and costs based on inundation depths were assigned to road sections.

The second group (highlighted in light blue) consisted on iteratively modeling the network functional capacity over time and running a recursive inspection and restoration algorithm described in Lam and Adey [18] to obtain the time-varying network states that were used in the third group of activities. In this group (highlighted in light orange), the degradation and recovery of traffic were modeled. This simulation was based on a macroscopic traffic model founded on the Method of Successive Averages [28] and a gravity-based Origin-Destination matrix founded on population data. Finally, the fourth group (highlighted in light green) calculated the probable direct consequences (i.e., costs that the network manager incurs; e.g., cost of restoration) and indirect consequences (i.e., costs that the network users incur; e.g., costs of traffic changes) during the hazard events and during the restoration periods. While direct consequences were estimated based on aggregated restoration costs, indirect consequences were quantified in terms of cost resulting from additional travel time through the network and missed trips.

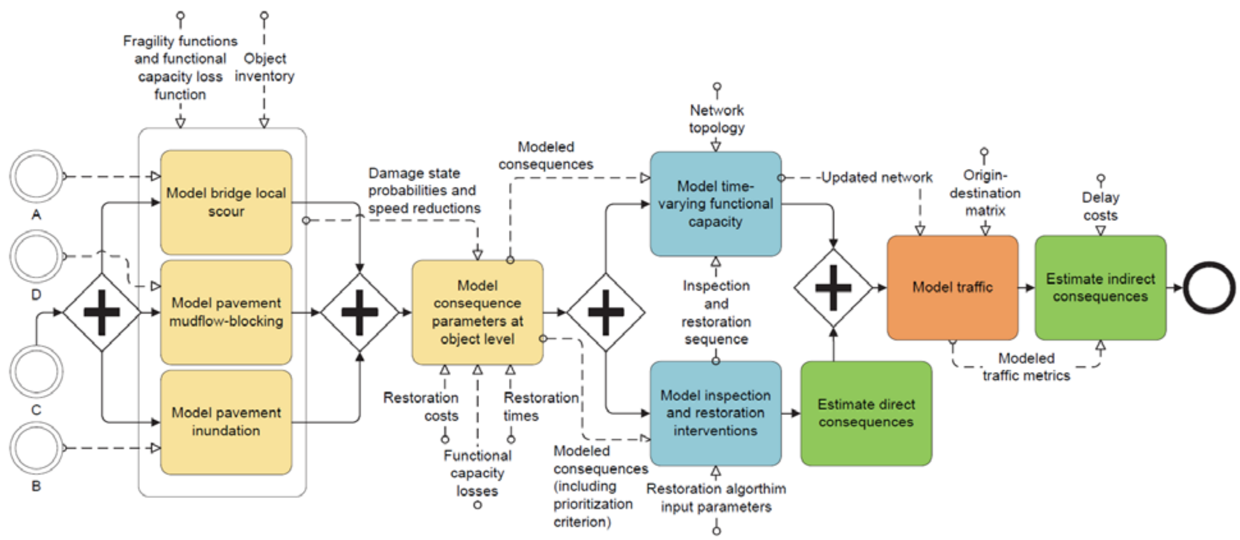

Figure 9 Damage and consequence sub-models

3.4. Stress test definition

The stress test conditions were:

- using 95-percentile fragility functions for bridge local scour and road section mudflow-blocking,
- using 95-percentile functional capacity loss functions for inundated road sections, and
- running 100 simulations of rainfall events with a 500-year return period.

While pavement sections are typically designed for up to 100-year return period events, bridge piers are generally designed for 500-year return period events. Selecting the former return period for the analysis would have resulted in the exclusion of bridge local scour as an object event as one could have deemed such a return period to be non-critical for that specific event. Selecting a return period higher than 500 years could have also been appropriate and such selection would have depended on other factors besides design return periods, including but not limited to an initiative to look specifically at events with relatively larger return periods (i.e., high-consequence, low-probability events).

This is an author generated post-print version (also known as "post-refereeing print" and "accepted manuscript") of the article:

Lam, J.C., Adey, B.T., Heitzler, M., Hackl, J., Gehl, P. , van Erp, N., D'Ayala, D., van Gelder, P., Hurni, L. (2018). Stress tests for a road network using fragility functions and functional capacity loss functions. Reliability Engineering & System Safety, 173, 78-93. 10.1016/j.ress.2018.01.015.

Note that some differences may be observed as a result of the copy-editing and typesetting process. The final manuscript is available on https://doi.org/10.1016/j.ress.2018.01.015. When citing this work, cite the final manuscript.

The evaluation criteria is presented in Table 4. The 2016 GDP was projected using data from the Federal Statistical Office [29].

Consequence indicator	**Consequence limit**	**Non-exceedance probability**	**Note on setting the consequence limit**
Cost of restoration	0.059% of the Canton of Grisons' 2016 GDP (i.e., CHF 8.48 million)	95%	High-income countries like Switzerland have maintained on low average annual loss-GDP ratio of 0.1% [30]. Although such a ratio is applicable to multiple hazard events, it should not be exceeded for a single set of cascading hazard events of 500-year return period. Moreover, through the analysis of the Swiss Federal Institute for Forest, Snow and Landscape Research's flood and landslide damage database [31], an average ratio of 59% was observed between the restoration costs of damaged road network objects, and the restoration costs of all damaged objects in the Canton of Grisons resulting from floods and debris flows.
Cost of additional travel time plus the cost of missed trips (i.e., costs of traffic changes)	1% of the Canton of Grisons' 2016 GDP (i.e., CHF 143.79 million)	95%	An average annual loss-GDP ratio of 1% is typically large enough to require risk-reducing interventions.

Table 4 Evaluation criteria

Note 4.1: Average annual loss was defined as the expected restoration cost of damaged objects per year averaged over a very long period of time when considering the probable hazard events that may occur during this period.

3.5. Fragility functions and functional capacity loss functions

This section briefly presents the fragility functions used for bridge local scour and road section mudflow-blocking, as well as the functional capacity loss functions for inundated road sections. The full description of the methods and data used for the development of the functions can be found in Hackl, Heitzler [1].

3.5.1. Fragility function for bridges local scour

Five bridges in the area of study were identified to be prone to local scour. Based on available data, these bridges were classified into two categories: (i) type A with one pier, and (ii) type B with two piers. Examples are presented in Figure 10.

Figure 10 Examples of bridges in the area of study of (left) type A and (right) type B

To construct the fragility functions for bridge local scour, the method proposed by Gehl and D’Ayala [32], D’Ayala, Gehl [15] and Gehl and D’Ayala [33] was used with several modifications (e.g., use of local scour equations found in Arneson, Zevenbergen [34] as opposed to those found in Richardson and Davis [35]). The damage states used in this analysis are described in Table 5. Due to lack of data, the damage states (i.e., ds_0, ds_1, ds_2, ds_3) were defined by comparing the calculated local scour depth (y_s) with a sampled percentage (i.e., x_1, x_2, x_3) of an assumed critical depth of local scour (i.e., level of scour where the bridge is not physically deemed to be safe for traffic; i.e., y_{cr}).

Damage state	Initial functional capacity loss	Threshold definition	Parameter definition
ds_0	No lane closure	$x_1 \cdot y_{cr} > y_s$	$y_{cr} \in \{unif(10,12)\ m\}$
ds_1	No lane closure	$x_2 \cdot y_{cr} > y_s \geq x_1 \cdot y_{cr}$	$x_1 \in \{unif(0.2,0.3)\}$
ds_2	Partial lane closure	$x_3 \cdot y_{cr} > y_s \geq x_2 \cdot y_{cr}$	$x_2 \in \{unif(0.45,0.55)\}$
ds_3	Full closure	$y_s \geq x_3 \cdot y_{cr}$	$x_3 \in \{unif(0.7,0.8)\}$

Table 5 Damage states for bridge local scour

A total of 100,000 points were estimated for each damage state, each of which represented a relationship between discharge and a probability of observing the same or higher damage state. These points were used to estimate the median (α) and dispersion (β) values for each fragility function using maximum likelihood estimation of binomial form with lognormally distributed failures. The results are presented in Table 6. The functions can be seen in Figure 11.

This is an author generated post-print version (also known as “post-refereeing print” and “accepted manuscript”) of the article:

Lam, J.C., Adey, B.T., Heitzler, M., Hackl, J., Gehl, P. , van Erp, N., D'Ayala, D., van Gelder, P., Hurni, L. (2018). Stress tests for a road network using fragility functions and functional capacity loss functions. Reliability Engineering & System Safety, 173, 78-93. 10.1016/j.ress.2018.01.015.

Note that some differences may be observed as a result of the copy-editing and typesetting process. The final manuscript is available on https://doi.org/10.1016/j.ress.2018.01.015. When citing this work, cite the final manuscript.

	Parameters for bridge type A		Parameters for bridge type B	
Symbol	95-percentile	50-percentile	95-percentile	50-percentile
α_{ds_1}	110	249	45	107
α_{ds_2}	2,411	4,170	993	1,706
α_{ds_3}	14,566	24,208	5,567	8,980
β_{ds_1}	0.45	0.66	0.41	0.64
β_{ds_2}	0.46	0.58	0.41	0.54
β_{ds_3}	0.50	0.61	0.43	0.54

Table 6 Local scour fragility function parameters for bridges of type A and type B

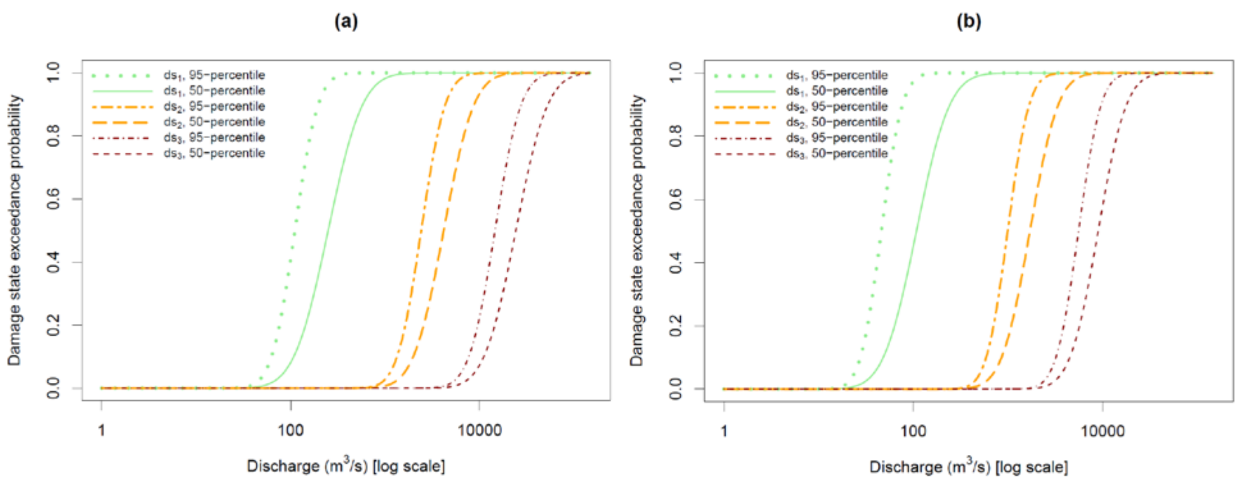

Figure 11 Bridge local scour fragility functions for bridges of (a) type A and (b) type B

3.5.2. Fragility functions for road section mudflow-blocking

To construct the fragility functions for road section mudflow-blocking, expert data were used from the survey conducted by Winter, Smith [36] and Winter, Smith [37]. Experts assigned probabilities of damage state exceedance to various combinations of pre-determined mudflow volumes and road section categories. Road sections were categorized into high-speed roads and local roads of 500 m each, and four damage states were defined as none (ds_0), limited (ds_1), serious (ds_2), and destroyed (ds_3) for each of these categories. These damage states were matched to functional capacity losses of no lane closure, partial lane closure, partial lane closure and full closure. Experts also provided information on their level of expertise, which served to weigh their responses.

For every combination of damage state and road category, four expert responses were iteratively and randomly sampled from the survey dataset. A maximum likelihood estimation of binomial form with lognormally distributed failures was performed to determine the corresponding fragility function median and dispersion values for each sampled survey set. A total of 10,000 median and dispersion values were estimated for every combination of damage state and road category. Assuming a lognormal distribution of these resulting values, the median and dispersion values for a fragility function of specific percentile were obtained. The results are presented in Table 7. The functions can be seen in Figure 12.

	Parameters for high-speed road sections		Parameters for local road sections	
Symbol	95-percentile	50-percentile	95-percentile	50-percentile
α_{ds_1}	472	8,670	215	2,216
α_{ds_2}	1,615	38,764	750	10,726
α_{ds_3}	4,184	98,856	2,297	17,790
β_{ds_1}	3.45	3.45	3.70	3.70
β_{ds_2}	2.92	2.92	3.31	3.31
β_{ds_3}	2.28	2.28	2.51	2.51

Table 7 Mudflow-blocking fragility function parameters for high-speed road and local road sections
Note 7.1: As suggested by Shinozuka, Feng [38], the dispersion value for a fragility function of any percentile is that of a 50-percentile fragility function.

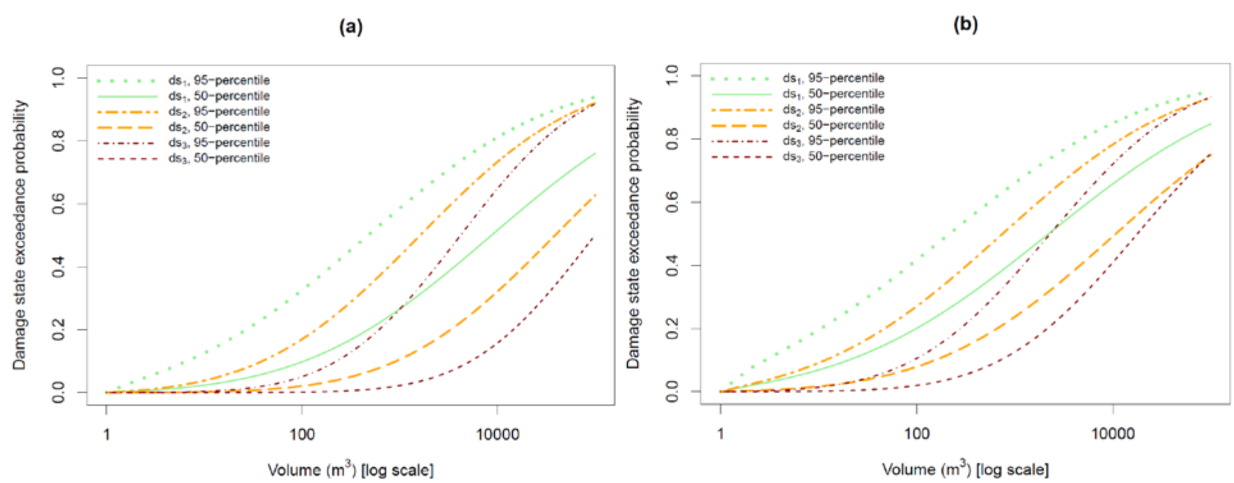

Figure 12 Road section mudflow-blocking fragility functions for (a) high-speed roads and (b) local roads

3.5.3. Functional capacity loss functions for bridge local scour and road section mudflow-blocking

The process proposed by Lam and Adey [18] was used to convert the derived fragility functions into functional capacity loss functions. Expected functional capacity losses were determined as functions of hazard intensities using the derived damage state probabilities and the (illustrative) functional capacity loss values for each damage state shown in Table 8. These values were either directly obtained or inferred from a survey conducted by D’Ayala, Gehl [15]. The resulting functional capacity loss functions were then used to support the estimation of the time-varying network functional capacity.

	Functional capacity loss (% closed lanes)	
Damage state	**Bridge local scour**	**Road section mudflow-blocking**
ds_1	0.0	0.3
ds_2	0.2	0.5
ds_3	1.0	1.0

Table 8 Functional capacity loss used for bridge local scour and road section mudflow-blocking
Note 8.1: For each object event, the values presented correspond to the initial functional capacity losses and functional capacity losses during restoration for all damage states (i.e., same values for both types of losses).

3.5.4. Functional capacity loss functions for road section inundation

A negative exponential function was used to model the relationship between inundation depth (D_{fld}) and the speed of vehicles on the road ($v_{feasible}$). The function is shown in Equation 2, and it was anchored at the maximum feasible speed on any given road (i.e., v_{max}), which was determined to be the speed on high-speed road with no inundation. The estimated values of parameter γ to develop the 95 and 50-percentile functional capacity loss functions were estimated to be 0.375 and 0.3 based on a curve fitting exercise using (illustrative) points of reference.

$$v_{feasible} = v_{max} \cdot e^{-(D_{fld} \cdot \gamma)} \qquad 2$$

The negative exponential function was used to determine the initial functional capacity loss [$E(FCL_x^S)$] given an inundation depth for high-speed and local road sections x with a specific speed limit (v_{limit}) as seen in Equation 3. In the case of local roads, the initial functional capacity loss could have only been observed when the allowed speed met or exceeded the feasible speed. The resulting 95 and 50-percentile initial functional capacity loss functions are shown in Figure 13.

$$E(FCL_x^S|D_{fld}) = max\left(0, v_{limit} - v_{feasible}\right)/v_{limit} \qquad 3$$

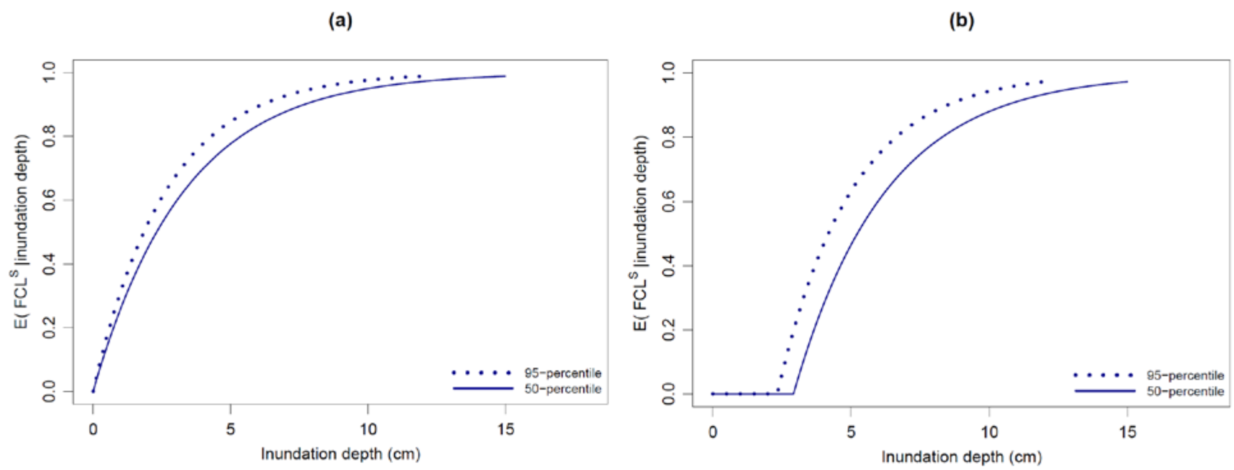

Figure 13 Road section inundation functional capacity loss functions for (a) high-speed roads and (b) local roads

During the restoration period, the functional capacity loss of a roads section was determined through a comparison between the maximum inundation level experienced (D_{fld}^{max}) and (illustrative) inundation thresholds ($D_{fld}^{level\,1}$, $D_{fld}^{level\,2}$) to determine whether an intervention was required. All of these values are listed in Table 9. This method, in particular, was a simplification that needs to be revisited in a subsequent analysis.

Required intervention	Functional capacity loss during restoration	Threshold definition	Parameter definition by percentile
No	No lane closure	$D_{fld}^{level\,1} > D_{fld}^{max}$	$D_{fld}^{level\,1,50\%} = 12\ cm$ $D_{fld}^{level\,1,95\%} = 15\ cm$
Yes	Partial lane closure	$D_{fld}^{level\,2} > D_{fld}^{max} \geq D_{fld}^{level\,1}$	$D_{fld}^{level\,2,50\%} = 24\ cm$
Yes	Full closure	$D_{fld}^{max} \geq D_{fld}^{level\,2}$	$D_{fld}^{level\,2,95\%} = 30\ cm$

Table 9 Levels of inundation with respect to interventions for road section inundation.

3.6. Cost of restoration and time to restore

The data used to estimate the expected restoration cost and time of bridges affected by local scour and road sections impacted by mudflows are presented in Table 10. These data were obtained directly or inferred from D’Ayala, Gehl [15]. Following the approach of Lam and Adey [18], these data were combined with the derived fragility functions to obtain restoration cost and restoration time functions to be used in the risk model.

This is an author generated post-print version (also known as "post-refereeing print" and "accepted manuscript") of the article:

Lam, J.C., Adey, B.T., Heitzler, M., Hackl, J., Gehl, P. , van Erp, N., D'Ayala, D., van Gelder, P., Hurni, L. (2018). Stress tests for a road network using fragility functions and functional capacity loss functions. Reliability Engineering & System Safety, 173, 78-93. 10.1016/j.ress.2018.01.015.

Note that some differences may be observed as a result of the copy-editing and typesetting process. The final manuscript is available on https://doi.org/10.1016/j.ress.2018.01.015. When citing this work, cite the final manuscript.

	Bridge local scour		Road section mudflow-blocking	
Damage state	Restoration cost (CHF/object)	Restoration time (days/object)	Restoration cost (CHF/km)	Restoration time (days/km)
ds_1	11,000	7	22,000	7
ds_2	55,000	30	55,000	7
ds_3	110,000	60	220,000	15

Table 10 Restoration cost and time data used for bridge local scour and road section mudflow-blocking
Note 10.1: Examples of restoration interventions for bridges include underpinning and scour protection.
Note 10.2: Examples of restoration interventions for road sections include debris removal, road repair, and slope mitigation measures.

The restoration costs (RC_{fld}) and times (RT_{fld}) for inundated road sections were estimated using piecewise functions—each with an exponential function embedded—that related these parameters to inundation depth. For this example, Equation 4 and Equation 5 were used to estimate restoration costs and restoration times using the data in Table 9 and Table 11.

$$RC_{fld} = \begin{cases} 0, & D_{fld} < D_{fld}^{level\,1} \\ {RC_{min}}^{a} \cdot {RC_{max}}^{b}, & D_{fld}^{level\,2} \geq D_{fld} \geq D_{fld}^{level\,1} \\ RC_{max}, & D_{fld} > D_{fld}^{level\,2} \end{cases}$$

$$where$$

$$a = \frac{\left(D_{fld}^{level\,2} - D_{fld}\right)}{\left(D_{fld}^{level\,2} - D_{fld}^{level\,1}\right)}$$

$$b = \frac{\left(D_{fld} - D_{fld}^{level\,1}\right)}{\left(D_{fld}^{level\,2} - D_{fld}^{level\,1}\right)} \quad (4)$$

$$RT_{fld} = \begin{cases} 0, & D_{fld} < D_{fld}^{level\,1} \\ {RT_{min}}^{a} \cdot {RT_{max}}^{b}, & D_{fld}^{level\,2} \geq D_{fld} \geq D_{fld}^{level\,1} \\ RT_{max}, & D_{fld} > D_{fld}^{level\,2} \end{cases} \quad (5)$$

Restoration cost		Restoration time	
Symbol	Value (CHF/object)	Symbol	Value (days/object)
RC_{min}	22,000	RT_{min}	30
RC_{max}	110,000	RT_{max}	120

Table 11 Restoration cost and time data used for road section inundation

Note 11.1: Examples of restoration interventions include roadwork to address design deficiencies, debris removal, traffic management measures, and drainage clearance.

3.7. Costs of traffic changes

The monetary values placed on an additional hour of travel time by network users was CHF 23.29, and on a missed trip was CHF 20.73 per hour times 16 hours on a given day—it was assumed that network users could miss the opportunity of traveling 16 of the 24 hours in a day. The hourly values were obtained from Schweizerischer Verband der Strassen- und Verkehrsfachleute [39].

4. Example results

The estimations for cost of restoration (Figure 14) ranged from CHF 0.45 million to CHF 11.83 million, and had an average of CHF 3.16 million and a median of CHF 2.16 million. The distribution was positively skewed and had a long tail.

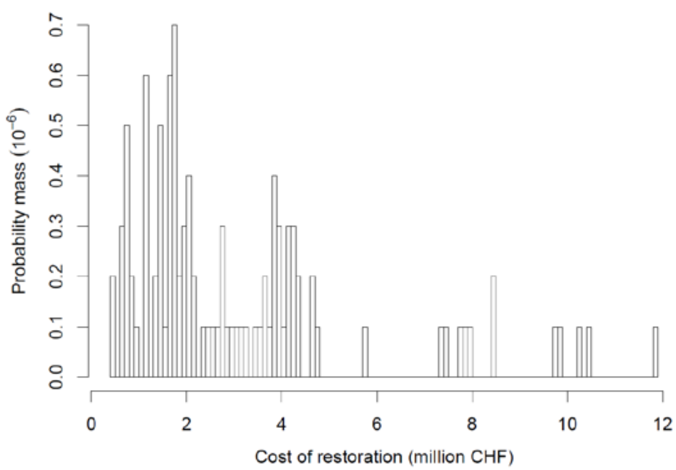

Figure 14 Distribution of the estimated cost of restoration for the stress test

The estimations for costs of traffic changes (Figure 15) ranged from CHF 2.90 million to CHF 218.15 million, and resulted in a mixture distribution with two modes. When examining the 100 observations, a jump between CHF 5.17 million and CHF 143.86 million is observed. This meant that while a small number of events—14 observations were equal or less than CHF 5.17 million—may result in damages, these events did not translate into significant traffic changes. In approximately half of these, the cost of restoration was less than CHF 0.85 million, and hence, low costs of traffic changes may be attributed to low level of damages. In the remaining instances, the costs of restoration amount up to CHF 4.36 million. For these cases, the damaged objects were not as critical as other objects with respect to the functioning of the network. For these 14 observations, the ratio between the cost of restoration and the costs of traffic changes averaged 0.477. For the remaining 86 observations, this ratio significantly decreased to 0.019.

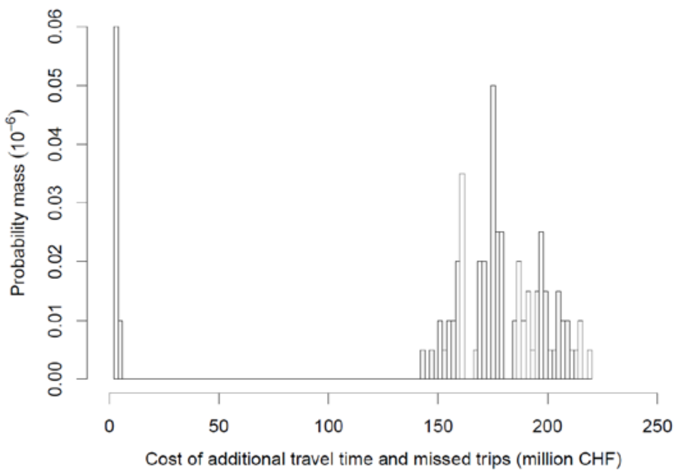

Figure 15 Distribution of the estimated costs of additional travel time and missed trips for the stress test

In the first-mode distribution (Figure 16), the cost estimates for traffic changes were slightly positively skewed, unlike the second-mode distribution where the estimates resembled a Gaussian distribution. For the first-mode distribution, the minimum value was CHF 2.90 million and the maximum was CHF 5.17 million. The mean was CHF 3.61 million and the median was CHF 3.46 million. No overall negative effects were observed (i.e., all costs are positive). Although benefits may be obtained in certain parts of the network at specific time steps during the hazard events period and restoration period due to missed trips, and hence, less congested routes, these benefits were far outweighed by the negative impacts in the remaining network and/or other time steps.

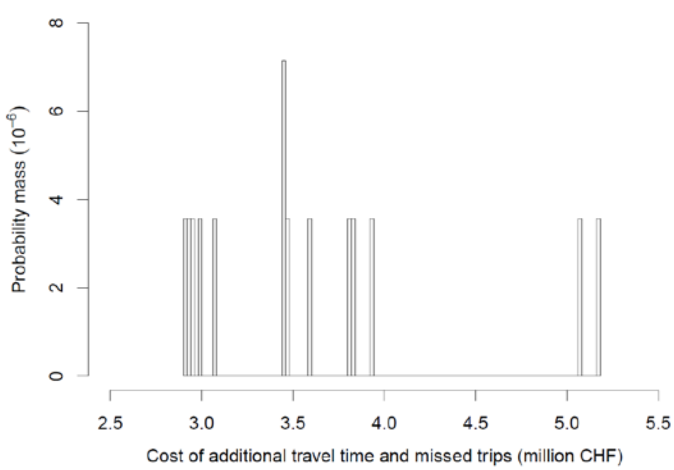

Figure 16 First-mode distribution of cost of additional travel time and missed trips for the stress test

For the second-mode distribution (Figure 17), the minimum cost was CHF 143.86 million and the maximum cost was CHF 218.15 million. The mean was CHF 180.73 million and the median was CHF 177.14 million. The number of days simulated for the 500-year return period events (corresponding to the second mode) ranged from 49 to 149. The minimum cost rate found in this mode was, therefore, CHF 1.15 million per day and the maximum calculated was CHF 3.05 million per day.

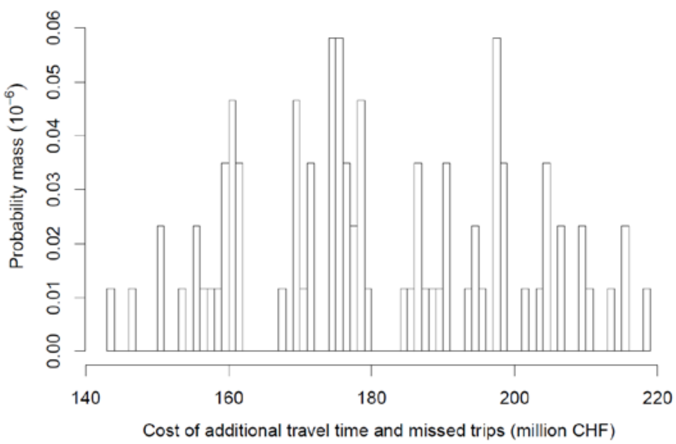

Figure 17 Second-mode distribution of cost of additional travel time and missed trips for the stress test

Parametric and non-parametric approaches can be used to approximate generalized distributions of the probable consequences. For this example, a non-parametric approach was used: distributions were approximated through log-transformed Gaussian kernel density estimates using Silverman’s rule of thumb for the selection of the bandwidth (please refer to Silverman [40] for more information). The log-transformation was implemented to avoid obtaining probable negative cost estimates, which would have implied benefiting from the occurrence of a rainfall and subsequent flood and mudflow events when such benefits could not have been possibly obtained. Figure 18 shows the non-parametric distributions related to the restoration of the network and the changes in traffic.

This is an author generated post-print version (also known as "post-refereeing print" and "accepted manuscript") of the article:

Lam, J.C., Adey, B.T., Heitzler, M., Hackl, J., Gehl, P. , van Erp, N., D'Ayala, D., van Gelder, P., Hurni, L. (2018). Stress tests for a road network using fragility functions and functional capacity loss functions. Reliability Engineering & System Safety, 173, 78-93. 10.1016/j.ress.2018.01.015.

Note that some differences may be observed as a result of the copy-editing and typesetting process. The final manuscript is available on https://doi.org/10.1016/j.ress.2018.01.015. When citing this work, cite the final manuscript.

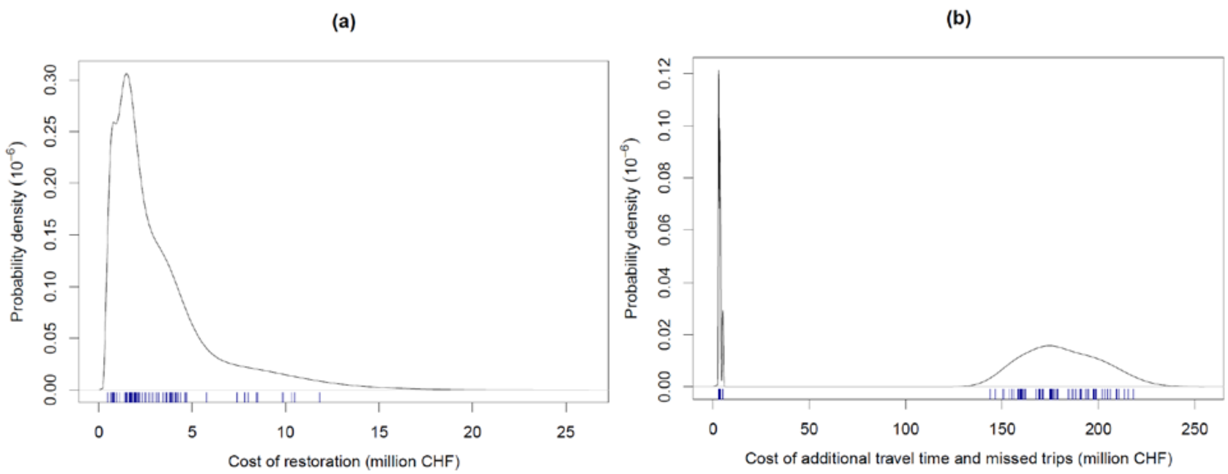

Figure 18 Non-parametric distributions of (a) the cost of restoration and (b) the cost of traffic changes for the stress test

The distribution of cost of restoration was positively skewed with a median value of CHF 2.35 million. It had a long tail with the 99-percentile value estimated at CHF 13.54 million. The 1-percentile value was estimated at CHF 0.42 million. As opposed to discretized distributions where the probabilities depend on the discrete cell sizes, density estimates are the result of a smoothing process, where points beyond those observed are assessed, and therefore, an analyst can expect to obtain a different set of probability estimates—please refer to differences in probability values between Figure 14 and Figure 18a.

With respect to the costs of traffic, this difference is more evident—please refer to differences in probability values between Figure 15 and Figure 18b. Furthermore, the density of the costs in the first mode with respect to the density of the costs in the second mode was more prominent in Figure 18b than in Figure 15, as if the density of the costs in the first mode were overestimated, or the density of the costs in the second mode were underestimated. Neither of these occurred, however. This is the effect of the smoothing process.

5. Example discussion

The estimated risks related to the restoration of the network and to the traffic changes are shown in Figure 19. In both cases, the non-exceedance probabilities of the consequence limit were lower than a 95%. The stress test was failed. At that point, however, the network manager could have decided to revise their risk model (i.e., better quantify uncertainty and reduce uncertainty). Such revision should not have targeted changes that support the passing of the stress test—in fact, changes may lead to larger estimated risk [41]. Some possible updates are:

- replacing key sub-models for more sophisticated and precise ones (at a computational expense in some cases),

- integrating data from additional field surveys that identify all bridges prone to local scour (and other types of scour) and characterize them in more detail (e.g., improved parameter distribution definition, improved bridge types, improved pier design description, improved critical levels of scour),
- enhancing the modeling of inundated pavements to best relate their functional capacity losses, restoration times and restoration costs, not solely as a function of inundation depth,
- harmonizing the collected survey results for functional capacity losses, restoration time and restoration costs,
- fitting probability distributions to the probable costs of restoration and the probable costs of traffic changes (as opposed to using Kernel estimates), and
- adding other types of hazard and object events that may be triggered by rainfall events.

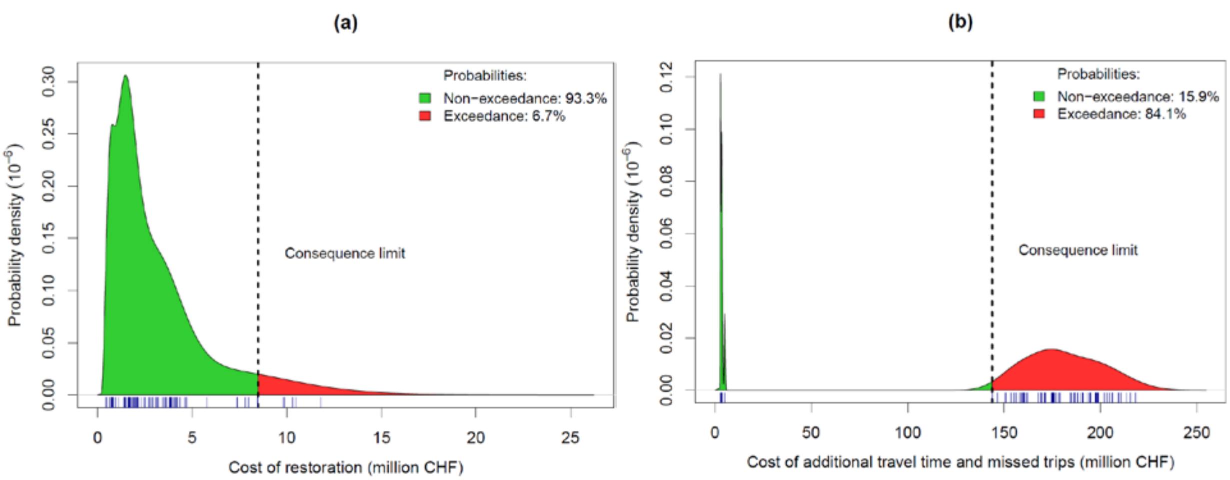

Figure 19 Stress test evaluation of adequate performance using (a) cost of restoration and (b) cost of traffic changes as consequence indicators

A revision of the risk model could have also occurred when considering the very low non-exceedance probability related to the costs of traffic changes (i.e., 15.9%). The network manager could have concluded (after careful consideration) that such costs were too high, and therefore, that the risk model required a revision.

As a point of comparison, the results when running the model using 50-percentile fragility and functional capacity loss functions are presented in Figure 20. While the estimated risks were lower than those obtained when using the 95-percentile functions (as expected), when using the same consequence limits to evaluate post-hazard performance, the network manager would still have implemented risk-reducing interventions because the non-exceedance probability related to the costs of traffic was still too low (i.e., 19.3%). If the network manager had originally based the decision to intervene solely on the costs of restoration works, then no interventions would have been implemented since the corresponding calculated non-exceedance probability was above 95%. It is then important for network managers to consider in their decision making processes the consequences absorbed by network users.

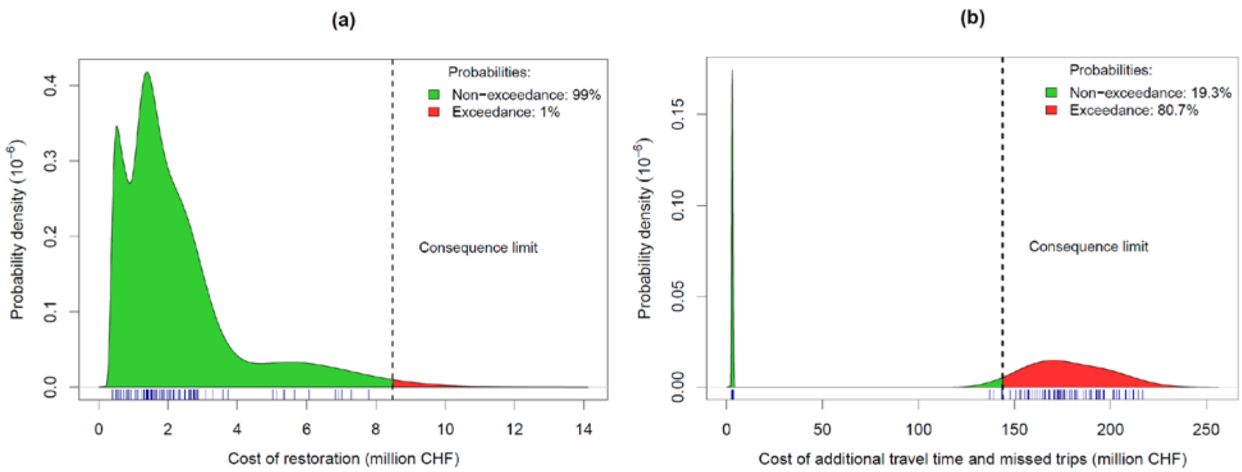

Figure 20 Evaluation of adequate performance using (a) cost of restoration and (b) cost of traffic changes as consequence indicators when using 50-percentile fragility and functional capacity loss functions

This comparison also showed that the relationship between direct and indirect consequences was not linear. The difference in non-exceedance probabilities between the conditioned and unconditioned model were 5.7% for the costs of restoration and 3.4% for the costs of traffic changes. In other words, an increase of restoration costs did not necessarily translate into a comparable increase of additional travel time and missed trips costs. Much more work is needed, however, including the analysis of results related to hazard events with other return periods, to best describe such a relationship.

For those interested in alternate visualizations of comparisons between the modeling results obtained when using 50-percentile fragility and functional capacity loss functions and the results obtained when using 95-percentile functions, please see the works of Heitzler, Lam [42] and Heitzler, Lam [43].

6. Conclusions

In this paper, a quantitative approach for conducting stress tests on road networks using fragility functions and functional capacity loss functions was presented. It was shown how traditional methods used in modeling the relationship between hazard events and object events can be used to determine if the post-hazard network performance is adequate. The probabilistic approach is suitable when evaluating the post-hazard performance of temporal and spatially distributed networks knowing that the events that need to be modeled to estimate risk are uncertain and can manifest in different ways over time and space. To demonstrate the application of the approach, an example was conducted for a road network in Switzerland exposed to floods as well as mudflows. The risk model used supported the estimation of probable costs of

This is an author generated post-print version (also known as "post-refereeing print" and "accepted manuscript") of the article:

Lam, J.C., Adey, B.T., Heitzler, M., Hackl, J., Gehl, P. , van Erp, N., D'Ayala, D., van Gelder, P., Hurni, L. (2018). Stress tests for a road network using fragility functions and functional capacity loss functions. Reliability Engineering & System Safety, 173, 78-93. 10.1016/j.ress.2018.01.015.

Note that some differences may be observed as a result of the copy-editing and typesetting process. The final manuscript is available on https://doi.org/10.1016/j.ress.2018.01.015. When citing this work, cite the final manuscript.

restoration and traffic changes. Both of these costs were used to determine whether risk-reducing interventions were to be executed. Table 12 summarizes the example.

Category	Description
Risk model	Road network was exposed to rainfall-triggered flood and mudflow events, leading to bridge local scour, mudflow-blocked road sections and inundated road sections, network functional capacity losses, restoration interventions and traffic changes (please see Table 2 and Table 3 for more information).
Stress test	The conditions applied to the risk model were: • 100 simulations of rainfall events with a 500-year return period, • 95-percentile fragility functions for bridge local scour and road section mudflow-blocking, and • 95-percentile functional capacity loss functions for inundated road sections The evaluation criteria was the following (please see Table 4 for additional details): • 95% probability that the cost of restoration will not exceed 0.059% of the Canton of Grison's 2016 GDP, or • 95% probability that the cost of traffic changes will not exceed 1% of the Canton of Grison's 2016 GDP
Stress test results	Risk-reducing interventions would need to be planned and executed given that the estimated non-exceedance probabilities were lower than the probabilities specified in the evaluation criteria. The results were: • 93.3% probability that the cost of restoration will not exceed 0.059% of the Canton of Grison's 2016 GDP, and • 15.9% probability that the cost of traffic changes will not exceed 1% of the Canton of Grison's 2016 GDP. Developing optimal work programs that include risk-reducing interventions is subject of future work, and so is the evaluation of other network management measures such as increasing emergency funds and enhancing restoration capabilities. Future work in this particular area may be built upon the work of Adey, Lethanh [44], Fernando, Adey [45], Lethanh and Adey [46], and Lethanh, Adey [47]. The evaluation of candidate work programs may also need to consider their likelihoods to succeed or fail [48].

Category	Description
Other possible actions	In addition to revising the risk model with the aim to better quantify the uncertainty or reduce the uncertainty (as suggested in the previous section), the network manager can consider: • reevaluating the decisions that led to the design of the stress test, and determine whether changes to the stress test are warranted (e.g., selecting rainfall events of different return period, increasing the number of rainfall simulations, using fragility functions and functional capacity loss functions of a different percentile), or • conducting additional stress tests that may consider other types of events such as hazard events (e.g., increasing the number of mudflow events) or societal events (e.g., decreasing the number of restoration crews, increasing the number of vehicles driving through the network to account for tourists during specific seasons).

Table 12 Summary of example

Despite the virtues of the approach presented here, there is still work to be done in the development of stress tests to support network managers in assessing post-hazard performance. Specifically, given the need to determine whether risk-reducing interventions are to be conducted using non-exceedance probabilities for consequence limits, it is necessary to evaluate further parametric and non-parametric approaches to represent the risk distribution. This is of special importance when a limited number of model simulations (i.e., limited number of risk estimations) is conducted given the considerable computational expense of risk models aiming to estimate probable direct and indirect consequences. In such an endeavor, future work has to look at the distribution of probable costs for various periods. Special attention should be given to the adequate representation of the right tails of the risk distributions, where the non-exceedance probabilities of consequence limits will likely be (e.g., probabilities above 90%) by evaluating the fitness of parametric and non-parametric functions in those locations.

On a broader level, future work should focus on investigating which stress tests should be used (e.g., which model conditions) in which situations (e.g., where these tests may yield benefits). This may require giving guidance on how to determine appropriate consequence indicators, consequence limits, and associated non-exceedance probabilities. At an operational level, this investigation may also demand the identification of suitable sub-models for the different types of stress tests and applications. All of these efforts would be conducive to the development of standards for conducting stress tests for networks—an area that is worth exploring to ease the implementation of stress tests in practice. Standards would also support the comparison of stress test results for different networks, bringing additional benefits to network managers (e.g., having the possibility to conduct benchmarking studies, improving the allocation of resources when resources are to be distributed to different networks). At the same time, a transition into a standard-supported environment may translate into enhanced financial protection mechanisms such more conservative amounts of contingency reserves, quicker access to these funds, and higher insurance coverage levels.

Acknowledgements

The work presented here has received funding from the European Union's Seventh Programme for Research, Technological Development and Demonstration under grant agreement No 603960, and from Horizon 2020, the European Union's Framework Programme for Research and Innovation, under grant agreement No 636285. The authors would like to thank the Research Unit of Geotechnical Earthquake Engineering and Soil Dynamics of the Aristotle University of Thessaloniki in Greece for granting access to the results of their expert survey used in the development of the mudflow-blocking fragility functions for high-speed and local road sections.

References

[1] Hackl J, Heitzler M, Lam JC, Adey BT, Hurni L. Final model, methodology and information exchange, deliverable 4.2. Novel indicators for identifying critical, INFRAstructure at RISK from Natural Hazards, grant agreement No 603960: ETH Zurich; 2016.
[2] Adey BT, Hajdin R, Birdsall J. Methodology to determine optimal intervention strategies for structures adversely affected by latent processes. Annual Conference of the Transportation Association of Canada. Vancouver, Canada: Transportation Association of Canada; 2009.
[3] van Erp HRN, Linger RO, Prak P, van Gelder PHAJM. Stress test framework for systems, deliverable 6.2. Novel indicators for identifying critical, INFRAstructure at RISK from Natural Hazards, grant agreement No 603960; 2016. p. 101.
[4] van Erp HRN, Linger RO, van Gelder PHAJM. Decision making protocol, deliverable 6.3. Novel indicators for identifying critical, INFRAstructure at RISK from Natural Hazards, grant agreement No 6039602016. p. 56.
[5] Li L, Yu Q, Bian Y, Yi P. Stress test of roadway network capacity. 2009 World Research Institutes World Congress on Computer Science and Information Engineering. Los Angeles, 2009. p. 467-71.
[6] Mercier A, Crozet Y, Ovtracht N, Buettner B, Wulfhorst G. Stress tests on urban mobility: Lessons for public policies. 13th World Conference on Transport Research. Rio de Janeiro, 2013.
[7] Lambert JH, Tsang JL, Thekdi SA. Risk-informed investment for tropical cyclone preparedness of highway signs, signals, and lights. Journal of Infrastructure Systems. 2013; 19:384-94.
[8] You H, Connelly EB, Lambert JH, Clarens AF. Climate and other scenarios disrupt priorities in several management perspectives. Environment Systems and Decisions. 2014; 34:540-54.
[9] Hamilton MC, Lambert JH, Valverde LJ. Climate and related uncertainties influencing research and development priorities. ASCE-ASME Journal of Risk and Uncertainty in Engineering Systems, Part A: Civil Engineering. 2015; 1:04015005.
[10] Thorisson H, Lambert JH, Cardenas JJ, Linkov I. Resilience analytics with application to power grid of a developing region. Risk Analysis. 2017; 37:1268-86.
[11] Avdeeva Y, van Gelder P. Stress test methodologies, deliverable 6.1. Novel indicators for identifying critical, INFRAstructure at RISK from Natural Hazards, grant agreement No 603960; 2014. p. 49.

[12] Zwicky P. Lessons learned from stress tests of nuclear facilities (Deliverable 2.1). WP2 – State-of-the-art and lessons learned; 2014. p. 52.
[13] European Nuclear Safety Regulators Group. Declaration of ENSREG, with annex EU stress test specifications. 2011.
[14] Clarke J, Lam JC, Gehl P, Taalab K, Corbally R. Risk assessment for an Italian road network due to an extreme earthquake hazard scenario and the associated landslide cascading effects. Civil Engineering Research in Ireland (CERI2016). Galway, Ireland: Civil Engineering Research Association of Ireland (CERAI); 2016.
[15] D'Ayala D, Gehl P, Martinovic K, Gavin K, Clarke J, Tucker M, et al. Fragility functions matrix, deliverable 3.2. Novel indicators for identifying critical, INFRAstructure at RISK from Natural Hazards, grant agreement No 603960; 2015. p. 167.
[16] Porter K. A beginner's guide to fragility, vulnerability, and risk. In: Beer M, Kougioumtzoglou AI, Patelli E, Au S-KI, editors. Encyclopedia of Earthquake Engineering. Berlin, Heidelberg: Springer Berlin Heidelberg; 2014. p. 1-29.
[17] Rossetto T, Ioannou I, Grant D, Maqsood T. Guidelines for empirical vulnerability assessment – Vulnerability Global Component Project. Pavia: GEM Foundation; 2014.
[18] Lam JC, Adey BT. Functional loss assessment and restoration analysis to quantify indirect consequences of hazards. ASCE-ASME Journal of Risk and Uncertainty in Engineering Systems, Part A: Civil Engineering. 2016; 2(4).
[19] Kermanshah A, Karduni A, Peiravian F, Derrible S. Impact analysis of extreme events on flows in spatial networks. 2014 IEEE International Conference on Big Data (Big Data), 2014. p. 29-34.
[20] Electric Power Research Institute. Seismic Fragility Application Guide. Palo Alto, CA: EPRI Technical Publishing; 2002. p. 210.
[21] Pregnolato M, Galasso C, Parisi F. A compendium of existing vulnerability and fragility relationships for flood: Preliminary results. Proceedings of the 12th International Conference on Applications of Statistics and Probability in Civil Engineering (ICASP12), Vancouver, Canada, July 12-15. 2015.
[22] National Institute of Building Sciences. Multi-hazard loss estimation methodology: Flood model HAZUS MH technical manual. Washington, DC: Federal Emergency Management Agency; 2003.
[23] Wüest M, Frei C, Altenhoff A, Hagen M, Litschi M, Schär C. A gridded hourly precipitation dataset for Switzerland using rain-gauge analysis and radar-based disaggregation. International Journal of Climatology. 2010; 30:1764-75.
[24] Kull DW, Feldman AD. Evolution of Clark's Unit Graph method to spatially distributed runoff. Journal of Hydrologic Engineering. 1998; 3:9-19.
[25] Losey S, Wehrli A. Schutzwald in der Schweiz: vom Projekt SilvaProtect-CH zum harmonisierten Schutzwald. Final Report. Bern, Switzerland: Switzerland: Bundesamt für Umwelt (BAFU); 2013.
[26] Zimmermann M, Mani P, Gamma P. Murganggefahr und Klimaänderung - ein GIS-basierter Ansatz. Zürich: vdf Hochschulverlag AG an der ETH Zürich, 1997.
[27] Hackl J, Heitzler M, Lam JC, Adey BT, Hurni L. Development of flood and mudflow events for the spatio-temporal risk assessment of networks. European Water. 2017; 57:179 - 85.
[28] Ortuozar JdD, Willumsen LG. Modelling transport. 4th ed.: John Wiley & Sons; 2011.

[29] Federal Statistical Office. Gross domestic product (GDP) per region and canton. National economy. Online: Federal Statistical Office; 2015.
[30] Cummins JD, Mahul O. Catastrophe risk financing in developing countries: Principles for public intervention. Washington, DC: World Bank; 2009.
[31] Hilker N, Badoux A, Hegg C. The Swiss flood and landslide damage database 1972–2007. Nat Hazards Earth Syst Sci. 2009; 9:913-25.
[32] Gehl P, D'Ayala D. Integrated multi-hazard framework for the fragility analysis of roadway bridges. Proceedings of the 12th International Conference on Applications of Statistics and Probability in Civil Engineering (ICASP12), Vancouver, Canada, July 12-15. 2015.
[33] Gehl P, D'Ayala D. Development of Bayesian Networks for the multi-hazard fragility assessment of bridge systems. Structural Safety. 2016; 60:37-46.
[34] Arneson LA, Zevenbergen LW, Lagasse PF, Clopper PE. Evaluating scour at bridges, 5th edition. Federal Highway Administration, editor. 2012.
[35] Richardson EV, Davis SR. Evaluating scour at bridges, 4th edition. Federal Highway Administration, editor. 2001.
[36] Winter MG, Smith JT, Fotopoulou S, Pitilakis K, Mavrouli O, Corominas J, et al. The physical vulnerability of roads to debris flow. 18th International Conference on Soil Mechanics and Geotechnical Engineering. Paris; 2013.
[37] Winter MG, Smith JT, Fotopoulou S, Pitilakis K, Mavrouli O, Corominas J, et al. An expert judgement approach to determining the physical vulnerability of roads to debris flow. Bull Eng Geol Environ. 2014; 73:291-305.
[38] Shinozuka M, Feng MQ, Kim H, Uzawa T, Ueda T. Statistical analysis of fragility curves. Buffalo: MCEER University at Buffalo, State University of New York; 2003.
[39] Schweizerischer Verband der Strassen- und Verkehrsfachleute, VSS-Fachkommission 1, Verkehrsplanung and VSS-Expertenkommission 1.02, Bewertungsverfahren. Kosten-Nutzen-Analysen im Strassenverkehr; Zeitkosten im Personenverkehr. SN 641 822a. Zürich, 2009.
[40] Silverman BW. Density estimation for statistics and data analysis. [Repr.] ed: Boca Raton : Chapman & Hall/CRC; 1998.
[41] Adey BT, Hackl J, Lam JC, van Gelder P, Prak P, van Erp N, et al. Ensuring acceptable levels of infrastructure related risks due to natural hazards with emphasis on conducting stress tests. 1st International Symposium on Infrastructure Asset Management. Kyoto, Japan: Kyoto University and Osaka University; 2016.
[42] Heitzler M, Lam JC, Hackl J, Adey BT, Hurni L. A simulation and visualization environment for spatio-temporal disaster risk assessments of network infrastructures. Cartographica: The International Journal for Geographic Information and Geovisualization 52, 2017, 349-363, 4.
[43] Heitzler M, Lam JC, Hackl J, Adey BT, Hurni L. GPU-accelerated rendering methods to visually analyze large-scale disaster simulation data. Journal of Geovisualization and Spatial Analysis. 2017; 1:3.
[44] Adey BT, Lethanh N, Kielhauser C. Comparison of three preventive maintenance models to determine optimal intervention strategies for transportation infrastructures in Alpine regions. International Journal of Architecture, Engineering and Construction. 2014; 3:153-67.

[45] Fernando D, Adey BT, Lethanh N. A model for the evaluation of intervention strategies for bridges affected by manifest and latent deterioration processes. Structure and Infrastructure Engineering: Maintenance, Management, Life-Cycle Design and Performance. 2014.
[46] Lethanh N, Adey BT. The use of MINLP to determine optimal preservation strategies for road links composed of pavement sections and bridges. In: F. Biondini, D.M. Frangopol, (Eds.), Bridge Maintenance, Safety, Management, Resilience and Sustainability, Proceedings of the Sixth International IABMAS Conference, Stresa, Lake Maggiore, Italy. 2012, 565-572.
[47] Lethanh N, Adey BT, Sigrist M. A mixed-integer linear model for determining optimal work zones on a road network. In: M. Papadrakakis MGK, N.D. Lagaros, editor. An International Conference on Engineering and Applied Sciences Optimization (OPTI 2014). Kos Island, Greece, 2014.
[48] Connelly EB, Thorisson H, Valverde LJ, Lambert JH. Asset risk management and resilience for flood control, hydropower, and waterways. ASCE-ASME Journal of Risk and Uncertainty in Engineering Systems, Part A: Civil Engineering. 2016; 2:04016001.